Composites Part B 120 (2017) 27–34

Contents lists available at ScienceDirect

Composites Part B

journal homepage: www.elsevier.com/locate/compositesb

Prediction of modulus at various strain rates from dynamic mechanical analysis data for polymer matrix composites

Steven Eric Zeltmann [a, *], Keerthana A. Prakash [a], Mrityunjay Doddamani [b], Nikhil Gupta [a]

[a] Composite Materials and Mechanics Laboratory, Mechanical and Aerospace Engineering Department, Tandon School of Engineering, New York University, Brooklyn, NY 11201, USA

[b] Advanced Manufacturing Laboratory, Department of Mechanical Engineering, National Institute of Technology Karnataka, Surathkal, India

ARTICLE INFO

Article history:
Received 20 February 2017
Received in revised form
27 March 2017
Accepted 28 March 2017
Available online 29 March 2017

Keywords:
Polymer-matrix composites (PMCs)
Thermoplastic resin
Analytical modeling
Mechanical testing

ABSTRACT

Understanding and modeling the behavior of polymers and composites at a wide range of quasi-static and high strain rates is of great interest to applications that are subjected to dynamic loading conditions. The Standard Linear Solid model or Prony series frameworks for modeling of strain rate dependent behavior are limited due to simplicity of the models to accurately represent a viscoelastic material with multiple relaxations. This work is aimed at developing a technique for manipulating the data derived from dynamic mechanical analysis to obtain an accurate estimate of the relaxation modulus of a material over a large range of strain rate. The technique relies on using the time-temperature superposition principle to obtain a frequency-domain master curve, and integral transform of this material response to the time domain using the theory of viscoelasticity. The relaxation function obtained from this technique is validated for two polymer matrix composites by comparing its predictions of the response to uniaxial strain at a prescribed strain rate to measurements taken from a separate set of tension experiments and excellent matching is observed.

1. Introduction

Dynamic mechanical analysis (DMA) is a widely used technique in the polymer science fields for characterizing thermal transitions in materials. It has traditionally been used primarily for the detection of thermal transitions, and associated properties such as glass transition temperature (T_g), polymer blend miscibility and composite interfacial bonding [1–10]. Recent works have focused on expanding the utility of the DMA technique to other applications such as to determine the properties of heterogeneous materials and for determination of crack location in composites [11–13]. In these existing cases, storage (E') and loss (E'') moduli measured through DMA are interpreted with respect to the material microstructure.

The focus of this work is to determine the strain rate sensitivity of materials by developing a transform to convert the frequency domain DMA results to time domain. Such a transform can significantly improve the usefulness of DMA results in materials and mechanics fields by providing the modulus at a wide range of strain rates, which is required in modeling and simulation studies on dynamic loading of structures. There are numerous difficulties in determining strain rate sensitivity using traditional testing. First, a large number of specimens are required to be tested at a wide range of strain rates. Second, universal testing machines do not have the response rates to measure load and deformations accurately at higher rates. This is particularly challenging in composite materials because the linear elastic region is often small and composites may undergo brittle failure before only a handful of data points can be captured at moderate strain rates. High strain rate properties of materials are studied experimentally [14–20] using techniques such as the tensile Hopkinson bar for use in analytical studies for structures and foams [21]. The use of multiple techniques for different strain rate regimes and unavailability of cross-correlation between properties obtained from quasi-static and dynamic test methods has emerged as a significant limitation. A central challenge to experimental characterization by traditional methods is that over small ranges of strain rate (a few orders of magnitude) many properties may appear to vary linearly with the logarithm of the strain rate (i.e. follow a power law) [22,23], while over a wider range this is usually not the case [24,25]. Extrapolation of the trends observed in the low-moderate strain rate regime to high strain rates can lead to significant error. This work explores the use of an

* Corresponding author.
E-mail address: steven.zeltmann@nyu.edu (S.E. Zeltmann).

http://dx.doi.org/10.1016/j.compositesb.2017.03.062
1359-8368/

alternative method for predicting strain rate sensitivity in polymers and composites: using time-temperature superposition (TTS) of dynamic mechanical analysis (DMA) data to determine the frequency domain response over a sufficiently wide range that it can be transformed to the time domain relaxation function.

Using the DMA transform technique of Zeltmann et al. [26], predictions of the strain rate sensitivity of the modulus of high density polyethylene (HDPE) matrix fly ash cenosphere reinforced composites called syntactic foams are computed and verified against results from tensile testing. Various properties of syntactic foams have been widely studied in the literature [27–29], and experimental studies are available on the high strain rate behavior of syntactic foams [30]. This method does not rely on an *a priori* form for the constitutive model, as often used in modeling strain rate sensitivity [31]. This work also explores further the application of the method, including using the Kramers-Kronig relations to compute an associated loss modulus function that provides a better indication of whether sufficient information has been captured to accurately represent the response. From the loss modulus master curve one can find the center of the transition, which can then be used to determine the critical strain rate at which the transition causes a significant curve in the strain rate sensitivity of viscoelastic properties.

This work aims at providing a resource for simulation and modeling efforts by providing a more sophisticated means of characterizing the dynamic response of the material and by correlating the elastic and viscoelastic properties. The results of the DMA transform technique can be utilized directly in many existing mechanical models [32–36] through the elastic-viscoelastic correspondence principle and for many other polymer matrix composites systems of interest [37–41].

This work uses fly ash hollow particles dispersed in HDPE to create a type of composite known as syntactic foam [42,43]. This class of composite materials has been widely studied for its mechanical properties and strain rate sensitivity [43,44]. Particulate composites such as the syntactic foams studied in this work are an ideal model system for exploring this transformation method because their mechanical properties are isotropic, so the properties measured in bending in the DMA are assumed to be the same as those measured in tension in the strain rate sensitivity experiments. Since the measurements are all taken on bulk properties, more complex systems such as those with viscoelastic fillers in a viscoelastic matrix are also able to be treated by this method, so long as they are within the linear elastic regime. Nevertheless, the transformation method discussed here is not limited to isotropic materials; in the case of anisotropy the material functions in different directions would be determined from separate measurements and combined using just as in the familiar theory of linear elasticity.

2. Experimental

2.1. Materials

HDPE of grade HD50MA180 supplied by Reliance Polymers, Mumbai, India, is used as the matrix material. The HDPE had a melt flow index of 20 g/10 min (190°C/2.16 kg) and a mean molecular weight of 97,500 g mol^{-1}. Cenospheres of CIL-150 grade, supplied by Cenosphere India Pvt. Ltd., Kolkata, India, are used as hollow fillers. Cenospheres are used in the as-received condition, without any surface treatment. Chemical, physical and sieve analysis results on the same type of cenospheres have been reported previously [45]. The cenospheres primarily comprise of alumina, silica, calcium oxide and iron oxides.

2.2. Sample fabrication

Cenospheres are used in 20 and 40 wt% in HDPE to fabricate two types of syntactic foams named HDPE20 and HDPE40, respectively, on a polymer injection molding (PIM) machine (Windsor, 80 ton capacity). Operating and processing parameters of the PIM machine were optimized in a set of earlier studies [23,46–48] and are set at 160 °C temperature and 30 kg/cm^2 (2.9 MPa) pressure. Samples of dimensions 60 × 12.7 × 3.3 mm^3 (length × width × height) are molded. The length of the specimens is later reduced by cutting with a diamond saw to 35 mm for DMA testing. Samples for tensile testing are also injection molded, with their geometry following ASTM D638.

2.3. Dynamic mechanical analysis

Dynamic mechanical analysis is conducted using a TA Instruments (New Castle, DE) Q800 DMA. Specimens are tested in the single cantilever configuration with a span length of 17.5 mm. Testing is conducted in the strain control mode with a maximum displacement of 25 μm. This displacement is achievable within the load limits of the machine at all temperatures for all the tested specimens. This ensures that the full specified strain is achieved throughout the entire test.

DMA testing is conducted in two phases: (a) using the temperature sweep mode at constant frequency of 1 Hz and (b) using the frequency sweep mode at a series of constant temperatures. In the temperature sweep test, the temperature is ramped from −100 °C to 130 °C at a rate of 1 °C/min. At least three specimens of each type are tested in this phase. In the frequency sweep testing, the temperature is stepped from −10 °C to 130 °C in increments of 5 °C. At each temperature step the specimen is soaked for 8 min to ensure thermal equilibrium. The dynamic properties are measured at 20 discrete frequencies logarithmically spaced between 1 and 100 Hz at each temperature step. Testing is halted if E' drops below 10 MPa, in order to prevent melting of the specimen in the clamp. At least three specimens of each type are tested in this phase. The results of temperature and frequency sweeping are combined using the time-temperature superposition (TTS) principle to generate master curves describing the behavior of syntactic foams over a wider range of frequencies.

2.4. Tensile testing

Tensile testing is conducted using an Instron 4467 universal test system. The specimen geometry conforms to ASTM D638. Strain data is collected using an Instron 1″ gage length extensometer attached to the test specimen. Tests are conducted with the crosshead speed set to give initial strain rates of 10^{-5}-10^{-2} s^{-1}, which are taken as the nominal strain rates for the tests. At least five specimens of each material type are tested at each strain rate.

2.5. Scanning electron microscopy

A Hitachi S3400 N scanning electron microscope is used for imaging of the syntactic foam microstructure. Specimens are sputter coated with gold using sputter coater to improve conductivity and prevent charging.

3. Results

Scanning electron micrographs of freeze-fractured surfaces of the syntactic foams are shown in Fig. 1. Fly ash cenospheres are observed to be distributed uniformly throughout the syntactic foam. Various factors such as matrix porosity entrapment, particle

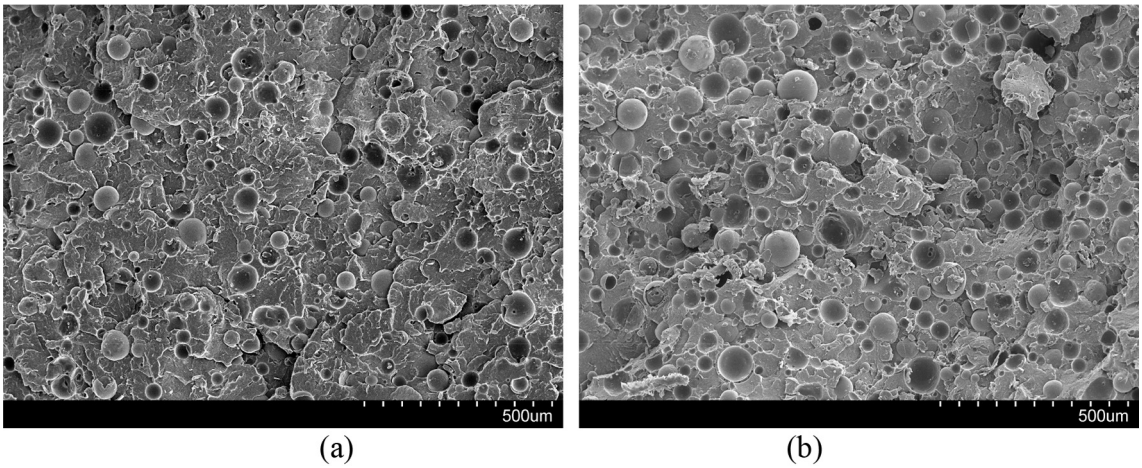

Fig. 1. Scanning electron micrographs of (a) HDPE20 and (b) HDPE40 freeze-fractured surfaces, showing uniform distribution of hollow particles. Particle fracture during processing does not appear to be significant.

crushing and quality of particle-matrix interface depend on the specimen fabrication method. These factors affect the mechanical properties, including elastic and viscoelastic properties, of syntactic foams. Extensive literature is available on all these factors for HDPE/cenosphere syntactic foams as well as numerous other types of syntactic foams. However, that information is not replicated here because the focus of this work is to examine if a transform can be developed to convert the frequency domain DMA results to time domain data to estimate the elastic modulus at various strain rates for these composites. Effect of various factors would be similar on tensile and DMA results and the developed transform should not be dependent on the material quality.

3.1. Tensile testing

A representative set of stress-strain curves for the HPDE resin are shown in Fig. 2 at 10^{-5} to 10^{-2} s^{-1} strain rates. These curves do not show distinct elastic and plastic regions. In addition, the effect of strain rate is clearly visible due to the viscoelastic nature of the material. Representative stress-strain curves for the HDPE/fly ash syntactic foams at strain rates from 10^{-5} to 10^{-2} s^{-1} are shown in Fig. 3. The syntactic foams show an initial nearly linear region up to about 0.5% strain, after which yielding occurs. The modulus in the initial elastic region and the yield stress increase with the strain rate, while the strain at yielding decreases. A more detailed analysis of the effect of processing parameters and composition on the tensile strength and failure strain can be found in the literature [46,47]. In syntactic foams, the matrix is usually assumed to be the only strain rate sensitive component, as the ceramic particles commonly used have insignificant damping compared to the matrix.

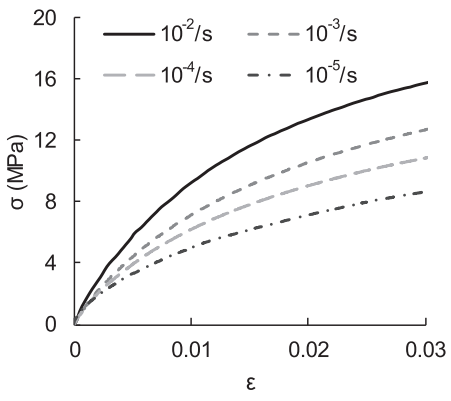

Fig. 2. Representative stress-strain curves for neat HDPE at various strain rates.

3.2. DMA temperature sweep

Results from the temperature sweep at 1 Hz are shown in Fig. 4 and Fig. 5 for HDPE20 and HDPE40, respectively. Both syntactic foams have a peak in the loss modulus at about 37 °C, which is due to the α-transition in HDPE [49]. Based on the loss modulus peak or the increase in tan δ, the onset of this transition is at about 0 °C. The transition continues until the HDPE is melted. At −100 °C there is evidence of another peak in the loss modulus, though the data do not include low enough temperatures to fully capture this peak. The peak in HDPE at −110 °C is generally associated with the glass transition. Since the HDPE is above its T_g and within the α-transition range at room temperature, strong strain rate sensitivity in its mechanical properties are expected.

3.3. DMA frequency sweep and time-temperature superposition

Following the temperature sweep, frequency sweeps are conducted from 1 to 100 Hz at stepped temperatures from −10 to 130 °C. A set of representative frequency sweeps for HDPE20 is presented in Fig. 6a. These frequency sweeps are combined using the time-temperature superposition (TTS) principle by shifting the various frequency sweeps along the frequency axis so that they form a single master curve [50]. No vertical shifting of the curves is employed in the TTS procedure. Representative master curves obtained for the two types of syntactic foams are shown in Fig. 6b. One step change in the storage modulus is observed in the master curve. The glass transition whose onset was observed at the lowest temperatures in the temperature sweep does not appear to have been captured here. Because the experiments are conducted using liquid nitrogen cooling, the total run time is limited. Since frequency sweeps require dwelling at constant temperature and substantial soaking times, the minimum temperature that can be reached before the cooling system is depleted is higher than for a constant frequency experiment.

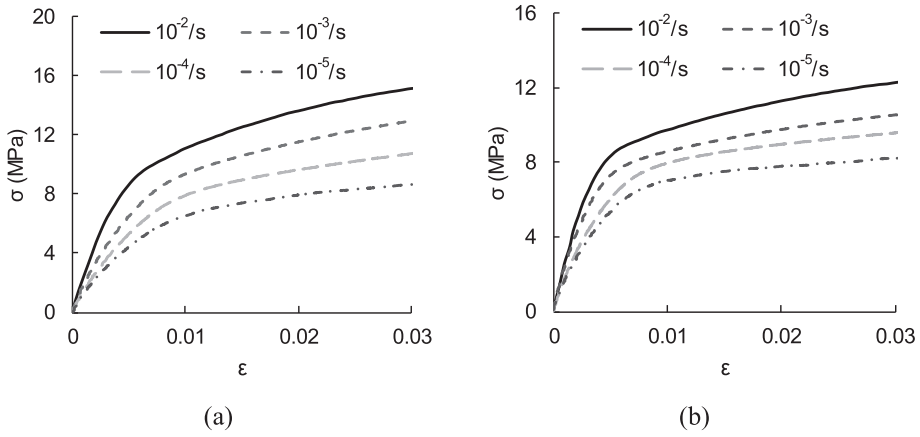

Fig. 3. Representative stress-strain curves for (a) HDPE20 and (b) HDPE40 at various strain rates.

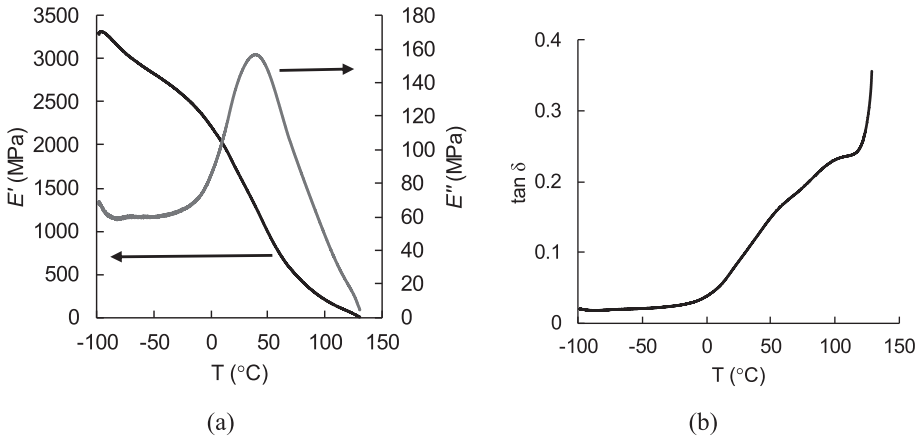

Fig. 4. Temperature sweep at 1 Hz for HDPE20 syntactic foam: (a) E' and E'' and (b) tanδ.

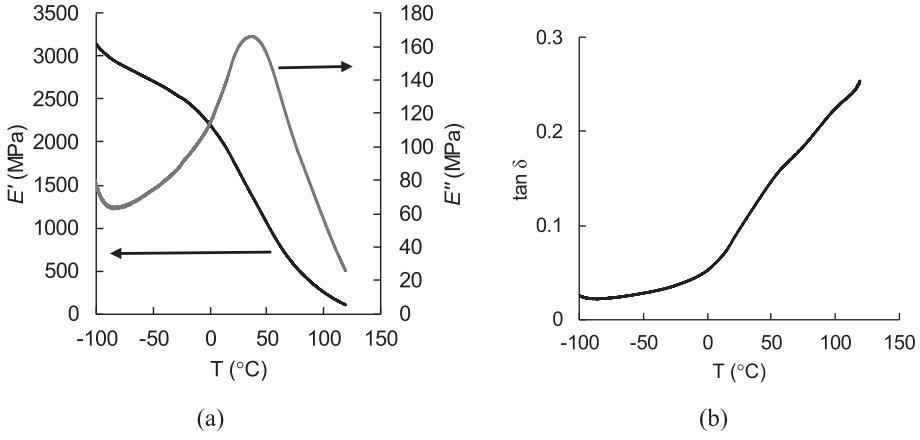

Fig. 5. Temperature sweep at 1 Hz for HDPE40 syntactic foam: (a) E' and E'' and (b) tanδ.

4. Discussion

4.1. Transformation to time-domain

Using the TTS principle, E' is found over a sufficiently wide range of frequencies to adequately characterize a viscoelastic function of the material. This frequency-domain viscoelastic function can, using an appropriate transformation, be converted to any of the other viscoelastic functions which may be more useful for engineering and design purposes. From E', and using the linear theory of viscoelasticity, the time domain relaxation modulus $E(t)$ can be found using [51]

$$E(t) = \frac{2}{\pi}\int_0^\infty \frac{E'(\omega)}{\omega}\sin(\omega t)d\omega \tag{1}$$

where ω and t represent angular frequency and time, respectively.

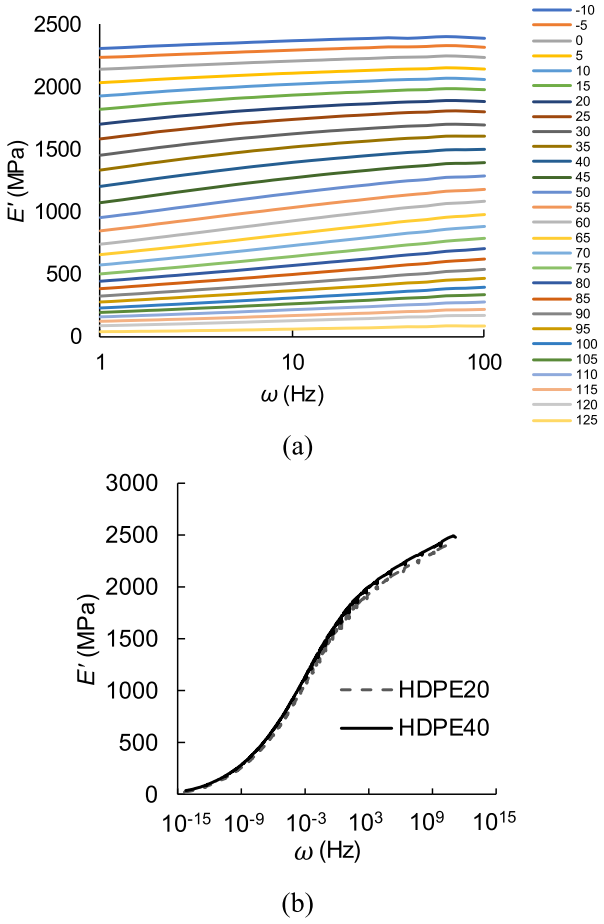

Fig. 6. (a) Representative set of frequency sweeps for HDPE20 and (b) storage modulus master curves constructed using 25 °C as the reference temperature for HDPE syntactic foams.

Since this is an improper integral, the experimental data must be extrapolated to zero and infinite frequencies. To do so the storage modulus master curve at a chosen temperature is fitted to a sigmoidal function of $\log(\omega)$ having the form

$$E'(\omega) = a\tanh(b(\log(\omega) + c)) + d \tag{2}$$

where a, b, c, and d are the fit coefficients and $\log(\omega)$ is the natural logarithm. The fit coefficients and the goodness of fit are given in Table 1. A fit of this form imposes that there is one smooth step transition in the E' curve, corresponding to one peak in E'', and that the behavior is asymptotic as frequency goes to zero or to positive infinity. For the case where the experimental data captures multiple transitions, a mixture of functions of this form can be applied, and the basis of the analysis in the following paragraphs would still apply. Such choice satisfies the physically required positive and bounded behavior of the relaxation function at zero and infinite frequencies [51] if $d > a$. However as the HDPE is above its T_g its behavior is like that of a viscoelastic liquid (i.e. $E'(\omega) = 0$) and fitting of the data yields $d \approx a$. The frequency at which $E'(\omega) = 0$, and below which E' is negative, is

$$\omega|_{E'=0} = \exp[\frac{-bc - a\tanh(d/a)}{b}] \tag{3}$$

which is of the order of 10^{-16} Hz for both syntactic foams. While it is simple to enforce that $E'(\omega) = 0$ in the curve fitting, this yields a poorer fit in the moderate frequency ranges which are most important to the response. In the unconstrained fit, the frequency at which the function is negative is sufficiently small that the negative E' will not substantially affect the resulting relaxation function, so the parameters from the unconstrained fit are used in the subsequent analysis.

The Kramers-Kronig (K-K) relations can be used to obtain the loss modulus function $E''(\omega)$ that corresponds to a given function for $E'(\omega)$ via the integral transform [52]

$$E''(\omega) = \frac{2\omega}{\pi}\int_0^\infty \frac{E'(\lambda) - E'(\omega)}{\lambda^2 - \omega^2}d\lambda \tag{4}$$

which can be approximated by

$$E''(\omega) \approx \frac{\pi}{2}\frac{dE'(\omega)}{d\ln\omega} \tag{5}$$

Though the transform could be integrated numerically, and more accurate but complex approximations exist [53], this simple form has been found to be widely applicable [51,54] and allows the use of an analytical form using the fitting function selected here. Based on the approximation of the Kramers-Kronig relations, the sigmoidal storage modulus function yields the loss modulus function

$$E''(\omega) = \frac{\pi ab}{2}\mathrm{sech}(b(\log(\omega) + c)^2 \tag{6}$$

which will be referred to as the "K-K prediction." The frequency at which this is maximal, ω_T, and which is the typical definition of the location of the transition, is found to be

$$\omega_T = \exp\left(\frac{1}{c}\right) \tag{7}$$

Thus one can obtain a frequency-temperature pair that corresponds to a transition. The transition temperature corresponding to this transition at another frequency can be found using the WLF equation and its experimentally determined coefficients [55]. Since transition temperatures are usually defined at 1 Hz, this method could be used to find transitions that are below the temperature range of the test equipment by using the higher frequency data and TTS to extend the range. The magnitude of the extension of the temperature range by this technique would depend on the TTS shift factors, which quantify the relationship between changes in frequency and changes in temperature. The shift factors outside the experimental temperature range can be estimated by the WLF [56] or Arrhenius equations, as applicable. The fit parameter b is related to the breadth, or "sharpness" of the transition.

The K-K prediction of the loss modulus curve is compared to the experimentally determined loss modulus master curves in Fig. 7. The loss modulus master curves are constructed by shifting the loss modulus curves from the frequency sweeps using the shift factors determined from shifting the storage modulus curves. At frequencies below the peak, excellent agreement is observed between the prediction and the master curve. However, above the peak the K-K prediction tends towards zero while the master curve remains

Table 1
Fit coefficients from the single-sigmoidal fit of the storage modulus master curve (Equation (2)), with E' in MPa and ω in radians/sec.

Material	a	b	c	d	R^2
HDPE20	1224.9	0.06155	3.6566	1167.3	0.9993
HDPE40	1276.1	0.05935	4.1236	1193.9	0.9992

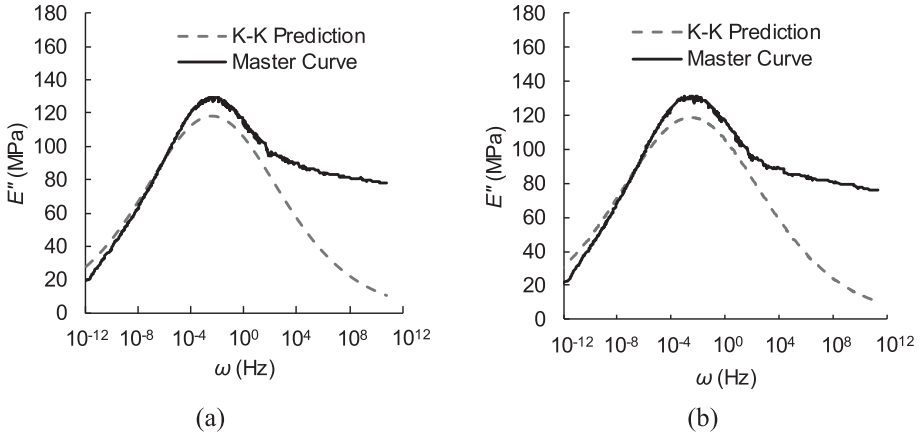

Fig. 7. Comparison of the experimental loss master curves at 25 °C with the predictions of the approximate K-K relations (Equation (6)), using the coefficients of the fit function for (a) HDPE20 and (b) HDPE40.

higher. This is likely due to the presence of another peak at higher frequencies (lower temperatures) than what was captured in the frequency sweep experiments. The use of the K-K prediction in comparison to the experimental loss modulus master curve is a more sensitive means to assess the goodness of fit, since transitions near the minimum and maximum frequency are difficult to discern from the storage modulus master curve. Such deviations appear clearly on the loss modulus master curve since the loss modulus shows peaks at these transitions.

The transform in Equation (1) is applied to the storage modulus fitting function by integrating numerically, to yield the time domain relaxation function for the material. The integral is the product of a positive and decreasing function with a sinusoid, so the improper integral can be converted to the summation of an alternating series whose terms are the integral evaluated between the zeroes of the sinusoid. An accelerated convergence approach can then be used to approximate the infinite summation.

The relaxation function generated using the room temperature master curve is shown in Fig. 8. The relaxation function can be observed to satisfy the requirements of fading memory and nonnegative stored and dissipated energy as expressed by Ref. [57]

$$E(t)\geq 0,\ dE(t)/dt \leq 0,\ d^2E(t)/dt^2 \geq 0 \tag{8}$$

within the range of times displayed. Since $d < a$ in the fitted functions, at some time the relaxation function will violate the first condition and yield a negative value for $E(t)$. However, this crossover is observed to happen at around 10^{14} s (about 3 million years), well beyond practical time scales.

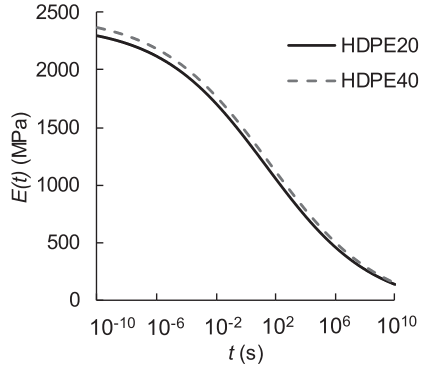

Fig. 8. Relaxation functions for HDPE syntactic foams at 25 °C.

The time-domain relaxation function determines the stress history generated by a specified strain history (for the one-dimensional case) according to [51]

$$\sigma(t) = E \times d\varepsilon = \int_{-\infty}^{t} E(t-\tau)\frac{d\varepsilon(\tau)}{d\tau}d\tau \tag{9}$$

where σ, ε and τ represent stress, strain and time variable used for integration, respectively. In anisotropic materials, this becomes a tensor expression (see Ref. [51]). However, we assume that the syntactic foams used in this work are isotropic as the reinforcing particles are spherical and uniformly distributed. In fiber-reinforced composites, DMA measurements would need to be performed in different orientations to build the relaxation function tensor, which could be used for arbitrary states of strain.

For constant strain rate deformation with a strain rate of $\dot{\varepsilon}$ beginning at $t = 0$, which is the idealized deformation state in a standard tension test, the convolution integral simplifies to

$$\sigma(t) = \dot{\varepsilon}\int_{0}^{t} E(\tau)d\tau \tag{10}$$

and the corresponding strain is obviously

$$\varepsilon(t) = \dot{\varepsilon}t \tag{11}$$

From this procedure, the linear viscoelastic response of the material at a constant strain rate can be determined. From the stress-strain relationship that results, relevant material properties can be derived.

Since the elastic response of HDPE is not perfectly linear, the predictions are compared with the results from tension experiments for HDPE matrix syntactic foams using the secant modulus at a prescribed strain. The 0.5% secant modulus derived from the DMA transform technique are compared with the results from the tension experiments in Fig. 9. The DMA transform line is shown only for one specimen but multiple specimens were tested and they showed consistent behavior. Excellent agreement is observed for both syntactic foams between the secant modulus and DMA transformation results. This method is not expected to be affected by factors such as imperfect interface in the composite, particles crushed during composite fabrication or air entrapment in the matrix because both the DMA measurements and the tensile test

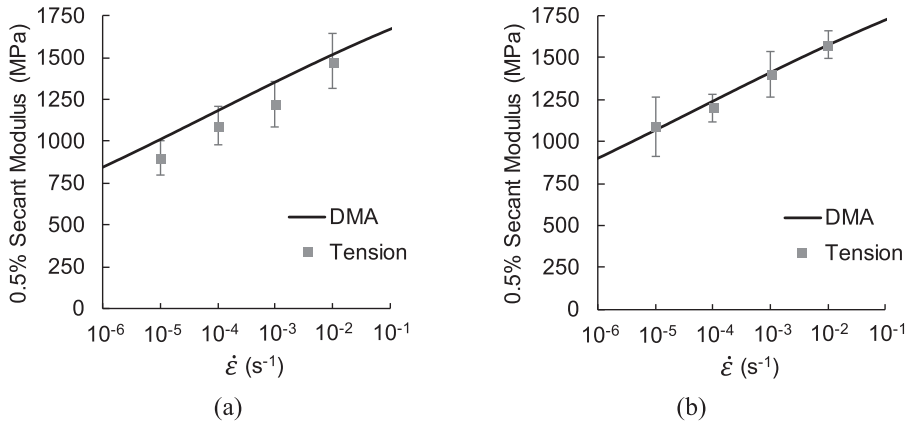

Fig. 9. Strain rate sensitivity of (a) HDPE20 and (b) HDPE40 compared to results from tensile experiments.

results will be affected similarly by such factors. Therefore, the DMA transformed results should still match with the tensile test data. In composites containing low volume fraction of particles, segregation of particles may be a concern that can provide a large variability in the test results. However, segregation or microstructural inhomogeneity would only require testing a larger number of specimens for both tests as per the routine statistical procedures due to large standard deviation values for a batch of specimens. Successful application of the transform developed in this work eliminates the need for conducting a large number of tensile test specimens at a wide range of strain rates. The curve of modulus with respect to strain rate captured through this transform can be used in modeling and simulation studies.

5. Conclusions

In this work, integral transform of dynamic mechanical data was used to convert the frequency spectrum obtained from time temperature superposition into a time domain relaxation function. Using the relaxation function, the linear viscoelastic response to a given strain history can be obtained. Predictions of the response in constant strain rate uniaxial deformation were compared to tension experiments and excellent agreement was observed. In addition, approximations to the Kramers-Kronig relations were used to obtain a well-matched estimate of the loss modulus master curve at frequencies up to the transition. Comparison of the loss master curve with the K-K prediction provides a better indication of the appropriateness of the fit function, as transitions near the edge of the experimental frequency range cause a small kink in the storage modulus curve versus peaks in the loss modulus.

Acknowledgements

This work is supported the Office of Naval Research Global N00014-10-1-0988. Authors acknowledge Dr. Keshav Prabhu, Mr. Puneeth and Mr. Praveen of Konkan Speciality Polyproducts Pvt. Ltd., Mangalore, Karnataka, India for providing the injection molding facility for sample fabrication. William Peng is thanked for useful mathematical discussions. Partial support from NYU Abu Dhabi Office of Research for Keerthana and NYUAD Dean of Engineering for Mrityunjay is acknowledged. The views expressed in this article are those of the authors, not of the funding agencies.

References

[1] Qiao J, Amirkhizi AV, Schaaf K, Nemat-Nasser S. Dynamic mechanical analysis of fly ash filled polyurea elastomer. J Eng Mater Technol 2010;133(1):011016–011016-7.
[2] Saba N, Jawaid M, Alothman OY, Paridah MT. A review on dynamic mechanical properties of natural fibre reinforced polymer composites. Constr Build Mater 2016;106:149–59.
[3] Jose S, Thomas S, Parameswaranpillai J, Aprem AS, Karger-Kocsis J. Dynamic mechanical properties of immiscible polymer systems with and without compatibilizer. Polym Test 2015;44:168–76.
[4] Jones DS. Dynamic mechanical analysis of polymeric systems of pharmaceutical and biomedical significance. Int J Pharm 1999;179(2):167–78.
[5] Chandra R, Singh SP, Gupta K. Damping studies in fiber-reinforced composites – a review. Compos Struct 1999;46(1):41–51.
[6] Poveda RL, Achar S, Gupta N. Viscoelastic properties of carbon nanofiber reinforced multiscale syntactic foam. Compos Part B Eng 2014;58:208–16.
[7] Yang S, Taha-Tijerina J, Serrato-Diaz V, Hernandez K, Lozano K. Dynamic mechanical and thermal analysis of aligned vapor grown carbon nanofiber reinforced polyethylene. Compos Part B Eng 2007;38(2):228–35.
[8] Yang F, Ou Y, Yu Z. Polyamide 6/silica nanocomposites prepared by in situ polymerization. J Appl Polym Sci 1998;69(2):355–61.
[9] Wang X, Hu Y, Song L, Yang H, Xing W, Lu H. In situ polymerization of graphene nanosheets and polyurethane with enhanced mechanical and thermal properties. J Mater Chem 2011;21(12):4222–7.
[10] Lin N, Chen G, Huang J, Dufresne A, Chang PR. Effects of polymer-grafted natural nanocrystals on the structure and mechanical properties of poly(-lactic acid): a case of cellulose whisker-graft-polycaprolactone. J Appl Polym Sci 2009;113(5):3417–25.
[11] Kostka P, Holeczek K, Höhne R, Filippatos A, Modler N. Extension and application of dynamic mechanical analysis for the estimation of spatial distribution of material properties. Polym Test 2016;52:184–91.
[12] Jia Z, Amirkhizi AV, Nantasetphong W, Nemat-Nasser S. Experimentally-based relaxation modulus of polyurea and its composites. Mech Time-Depend. Mater 2016;20(2):155–74.
[13] Nielsen C, Nemat-Nasser S. Crack healing in cross-ply composites observed by dynamic mechanical analysis. J Mech Phys Solids 2015;76:193–207.
[14] Song B, Chen WW, Lu WY. Mechanical characterization at intermediate strain rates for rate effects on an epoxy syntactic foam. Int J Mech Sci 2007;49(12):1336–43.
[15] Yoon, S.-h. and Siviour, C.R., Application of the virtual fields method to a relaxation behaviour of rubbers. J Mech Phys Solids.
[16] Zhou Y, Akanda SR, Jeelani S, Lacy TE. Nonlinear constitutive equation for vapor-grown carbon nanofiber-reinforced SC-15 epoxy at different strain rate. Mater Sci Eng A 2007;465(1–2):238–46.
[17] Jia Z, Hui D, Yuan G, Lair J, Lau K-t, Xu F. Mechanical properties of an epoxy-based adhesive under high strain rate loadings at low temperature environment. Compos Part B Eng 2016;105:132–7.
[18] Hao X, Kaschta J, Schubert DW. Viscous and elastic properties of polylactide melts filled with silica particles: effect of particle size and concentration. Compos Part B Eng 2016;89:44–53.
[19] Zhang B, Lin Y, Li S, Zhai D, Wu G. Quasi-static and high strain rates compressive behavior of aluminum matrix syntactic foams. Compos Part B Eng 2016;98:288–96.
[20] Peroni L, Scapin M, Fichera C, Lehmhus D, Weise J, Baumeister J, et al. Investigation of the mechanical behaviour of AISI 316L stainless steel syntactic foams at different strain-rates. Compos Part B Eng 2014;66:430–42.
[21] Romero PA, Zheng SF, Cuitiño AM. Modeling the dynamic response of viscoelastic open-cell foams. J Mech Phys Solids 2008;56(5):1916–43.
[22] Luong DD, Pinisetty D, Gupta N. Compressive properties of closed-cell polyvinyl chloride foams at low and high strain rates: experimental investigation and critical review of state of the art. Compos Part B Eng 2013;44(1):403–16.
[23] Bharath Kumar BR, Singh AK, Doddamani M, Luong DD, Gupta N. Quasi-static and high strain rate compressive response of injection-molded cenosphere/

HDPE syntactic foam. JOM 2016;68(7):1861–71.
[24] Sarva SS, Deschanel S, Boyce MC, Chen W. Stress–strain behavior of a polyurea and a polyurethane from low to high strain rates. Polymer 2007;48(8):2208–13.
[25] Luong DD, Shunmugasamy VC, Strbik III OM, Gupta N. High strain rate compressive behavior of polyurethane resin and polyurethane/Al_2O_3 hollow sphere syntactic foams. J Compos 2014;2014(795984):1–10.
[26] Zeltmann SE, Bharath Kumar BR, Doddamani M, Gupta N. Prediction of strain rate sensitivity of high density polyethylene using integral transform of dynamic mechanical analysis data. Polymer 2016;101:1–6.
[27] Nian G, Shan Y, Xu Q, Qu S, Yang Q. Failure analysis of syntactic foams: a computational model with cohesive law and XFEM. Compos Part B Eng 2016;89:18–26.
[28] Huang R, Li P. Elastic behaviour and failure mechanism in epoxy syntactic foams: the effect of glass microballoon volume fractions. Compos Part B Eng 2015;78:401–8.
[29] Tagliavia G, Porfiri M, Gupta N. Influence of moisture absorption on flexural properties of syntactic foams. Compos Part B Eng 2012;43(2):115–23.
[30] Huang R, Li P, Wang Z, Liu T. X-ray microtomographic characterization and quantification of the strain rate dependent failure mechanism in cenosphere epoxy syntactic foams. Adv Eng Mater 2016;18(9):1550–5.
[31] Buckley CP, Dooling PJ, Harding J, Ruiz C. Deformation of thermosetting resins at impact rates of strain. Part 2: constitutive model with rejuvenation. J Mech Phys Solids 2004;52(10):2355–77.
[32] Porfiri M, Gupta N. Effect of volume fraction and wall thickness on the elastic properties of hollow particle filled composites. Compos Part B Eng 2009;40(2):166–73.
[33] Bardella L, Genna F. On the elastic behavior of syntactic foams. Int J Solids Struct 2001;38(40–41):7235–60.
[34] Bardella L, Sfreddo A, Ventura C, Porfiri M, Gupta N. A critical evaluation of micromechanical models for syntactic foams. Mech Mater 2012;50:53–69.
[35] Nguyen VT, Hwu C. Holes, cracks, or inclusions in two-dimensional linear anisotropic viscoelastic solids. Compos Part B Eng 2017;117:111–23.
[36] Fedorov VA, Barkanov EN. Homogenisation of viscoelastic damping in unidirectional composites under longitudinal shear. Compos Part B Eng 2017;113:72–9.
[37] Liu H, Dong M, Huang W, Gao J, Dai K, Guo J, et al. Lightweight conductive graphene/thermoplastic polyurethane foams with ultrahigh compressibility for piezoresistive sensing. J Mater Chem C 2017;5(1):73–83.
[38] Liu H, Gao J, Huang W, Dai K, Zheng G, Liu C, et al. Electrically conductive strain sensing polyurethane nanocomposites with synergistic carbon nanotubes and graphene bifillers. Nanoscale 2016;8(26):12977–89.
[39] Petrie KG, Osazuwa O, Docoslis A, Kontopoulou M. Controlling MWCNT partitioning and electrical conductivity in melt compounded polypropylene/poly(ethylene-co-octene) blends. Polymer 2017;114:231–41.
[40] Zhang X, Gao H, Guo M, Li G, Liu Y, Li D. A study on key technologies of unmanned driving. CAAI Trans Intell Technol 2016;1(1):4–13.
[41] Alippi C. A unique timely moment for embedding intelligence in applications. CAAI Trans Intell Technol 2016;1(1):1–3.
[42] Labella M, Zeltmann SE, Shunmugasamy VC, Gupta N, Rohatgi PK. Mechanical and thermal properties of fly ash/vinyl ester syntactic foams. Fuel 2014;121:240–9.
[43] Rohatgi P, Weiss D, Gupta N. Applications of fly ash in synthesizing low-cost MMCs for automotive and other applications. JOM Journal of the Minerals, Metals Mater Soc 2006;58(11):71–6.
[44] Shunmugasamy VC, Gupta N, Nguyen NQ, Coelho PG. Strain rate dependence of damage evolution in syntactic foams. Mater Sci Eng A 2010;527(23):6166–77.
[45] Bharath Kumar BR, Doddamani M, Zeltmann SE, Gupta N, Ramesh MR, Ramakrishna S. Data characterizing tensile behavior of censophere/HDPE syntactic foam. Data Brief 2016;6:933–41.
[46] Bharath Kumar BR, Doddamani M, Zeltmann SE, Gupta N, Ramesh MR, Ramakrishna S. Processing of cenosphere/HDPE syntactic foams using an industrial scale polymer injection molding machine. Mater Des 2016;92:414–23.
[47] Bharath Kumar BR, Zeltmann SE, Doddamani M, Gupta N, Uzma, Gurupadu S, et al. Effect of cenosphere surface treatment and blending method on the tensile properties of thermoplastic matrix syntactic foams. J Appl Polym Sci 2016;133(35):1–11.
[48] Bharath Kumar BR, Doddamani M, Zeltmann SE, Gupta N, Uzma, Gurupadu S, et al. Effect of particle surface treatment and blending method on flexural properties of injection-molded cenosphere/HDPE syntactic foams. J Mater Sci 2016;51(8):3793–805.
[49] Khanna YP, Turi EA, Taylor TJ, Vickroy VV, Abbott RF. Dynamic mechanical relaxations in polyethylene. Macromolecules 1985;18(6):1302–9.
[50] Williams ML, Landel RF, Ferry JD. The temperature dependence of relaxation mechanisms in amorphous polymers and other glass-forming liquids. J Am Chem Soc 1955;77(14):3701–7.
[51] Christensen RM. Theory of viscoelasticity: an intoduction. New York: Academic Press; 1982.
[52] Booij HC, Thoone GPJM. Generalization of Kramers-Kronig transforms and some approximations of relations between viscoelastic quantities. Rheol Acta 1982;21(1):15–24.
[53] Brather A. Numerisch einfache Beziehungen zwischen Verlust- und Speicherkomponente des dynamischen Schermoduls und der dynamischen Nachgiebigkeit. Rheol Acta 1978;17(4):325–41.
[54] Schapery RA, Park SW. Methods of interconversion between linear viscoelastic material functions. Part II—an approximate analytical method. Int J Solids Struct 1999;36(11):1677–99.
[55] Shunmugasamy VC, Pinisetty D, Gupta N. Viscoelastic properties of hollow glass particle filled vinyl ester matrix syntactic foams: effect of temperature and loading frequency. J Mater Sci 2013;48(4):1685–701.
[56] Ferry JD. Viscoelastic properties of polymers. New York: John Wiley & Sons, Inc; 1961.
[57] Christensen RM. Restrictions upon viscoelastic relaxation functions and complex moduli. Trans Soc Rheol. 1972;16(4):603–14.